Radial Propagation of Turbulent Transport Events in the Scrape-Off Layer of Alcator C-Mod

O. Grulke 1), J. L. Terry 2), B. LaBombard 2), S. J. Zweben 3)

1) Max-Planck Institute for Plasma Physics, EURATOM Association,
D-17491 Greifswald, Germany
2) MIT Plasma Science and Fusion Center, Cambridge, MA 02139, USA,
3) Princeton Plasma Physics Laboratory, P.O. Box 451, Princeton, New Jersey 08540, USA

e-mail contact of main author: olaf.grulke@ipp.mpg.de

Abstract. This paper reports on investigations of propagating turbulent spatiotemporal structures in the scrape-off layer (SOL) of Alcator C-Mod. Structures are diagnosed using turbulence imaging techniques. A radial array of views coupled to diodes filtered for D_α and a fast framing camera system viewing D_α emission intensity in a poloidal-radial cross section utilize "gas-puff-imaging" to visualize the turbulence. The fluctuations display intermittence with fluctuation events propagating radially outwards through the entire SOL, thereby causing strongly asymmetric probability distribution functions. Wavelet analysis of the poloidal wavevector spectrum shows that the size scale of structure with significant spectral power is limited to the small-k regime. The temporal evolution of the poloidal wavevector spectrum shows the intermittent occurrence of these large events. Based on correlation analysis of the two-dimensional imaging data, the poloidal velocity is most likely determined by the background ExB drift. In the mid-SOL fluctuations propagate mainly in radial direction. For quantification of the propagation speeds the camera images are decomposed into large-amplitude fluctuation structures, which are tracked across the camera's field of view. The number distribution of radial velocities reveal that more than 80% of structures propagate radially outwards over distances larger than the typical structure size. The mean velocity is less than 1% of the ion sound speed, which is much smaller than predicted by basic structure propagation models. An increase of the radial structure velocity with peak structure amplitude is observed.

1. Introduction

A distinct feature of turbulence in the scrape-off layer (SOL) of tokamaks is the formation of intermittent spatiotemporal fluctuation structures, commonly called 'blobs' [1], which form in the strong plasma pressure gradient region close to the last closed flux surface. These structures have attracted special attention due to the associated cross-field transport [2,3], which is of particular importance in magnetically confined plasma and affects key reactor issues like heat deposition on material surfaces, first wall sputtering and recycling, and helium pumping. It is generally observed that blobs are fairly spatially localized in the poloidal plane but extend over much longer distances along the magnetic field, thereby forming flute-like filaments [4]. The transport caused by blobs is a direct consequence of their propagation characteristics. The propagation is not only in poloidal direction, i.e. the direction of the background plasma drifts, but they show also a strong radial component of propagation, which is connected to the self-consistent electric and magnetic fields local to the blob. The radial blob propagation has not only been observed in tokamak SOLs but also in laboratory experiments [5] and thus seems to be an universal feature. This multidimensional propagation makes the experimental investigation of blobs a challenging task and requires spatiotemporal diagnostics with high spatial and temporal resolution.
Although the details of the formation processes of blobs are under intense scientific debate, several models have been proposed to gain a better understanding of the radial propagation mechanism [6,7,8]. They usually rely on the curvature of the magnetic field, which either leads to polarization of the blob or to interchange dynamics. Although these models differ

fundamentally both approaches have in common that the increased plasma pressure of the blob is associated with a poloidally oriented dipole potential structure, which gives rise to a radial ExB drift. The dipole potential has been experimentally verified [4] and seems to be the primary reason for the radial propagation of the blob. In the context of cross-field transport the scaling of the radial blob velocity is of particular importance. The model predictions are based on characteristic blob features like relative fluctuation amplitude and spatial size, and configurational parameters like the magnetic field strength/curvature and connection length to material boundaries and differ significantly.

In the present paper we present detailed investigations of the spatiotemporal dynamics of turbulent fluctuation structures in the SOL of Alcator C-Mod using gas-puff imaging diagnostics (GPI). Special attention is paid to the radial propagation speed of large-amplitude fluctuation structures and its scaling with blob amplitude. The paper is organized as follows: in Sec. 2 the experimental configuration and diagnostic setup is outlined. Sec. 3 deals with the amplitude and spatial scales based on wavelet analysis of SOL fluctuations. The blob propagation characteristics and its scaling with amplitude is presented in Sec. 4 before the results are summarized in Sec. 5.

2. Experimental setup and gas-puff imaging diagnostics

Experiments presented here were done in Ohmic L-mode discharges in lower single-null configuration. The magnetic field configuration was chosen for a relatively large gap (typically ~ 2cm) between the last closed flux surface (LCFS) and the poloidal limiter edge, measured at the outer midplane. The toroidal magnetic field on axis was B=5.4T and the plasma current was I=630kA, which results in a safety factor of the 95% flux surface of $q_{95} \approx 6$. The average plasma density was chosen at moderate values of approx. 30% of the Greenwald density limit. A series of four discharges with nearly identical magnetic field configuration and plasma parameters are available, which improves the statistical confidence of the fluctuation analysis. Time-averaged SOL profiles are measured with a multi-tip reciprocating Langmuir probe. The primary fluctuation diagnostics used is the gas-puff imaging (GPI) technique [9,10,11]. It is based on the method to localize the emission (D_α in the present experiments) in toroidal dimension by a localized gas puff, which yields a strong increase of the emission intensity compared to the intrinsic emission along the line-of-sight. In C-Mod a gas puff is available on the outer midplane. The D_α emission is viewed tangentially to the local magnetic field with two complementary diagnostics. One of these is a

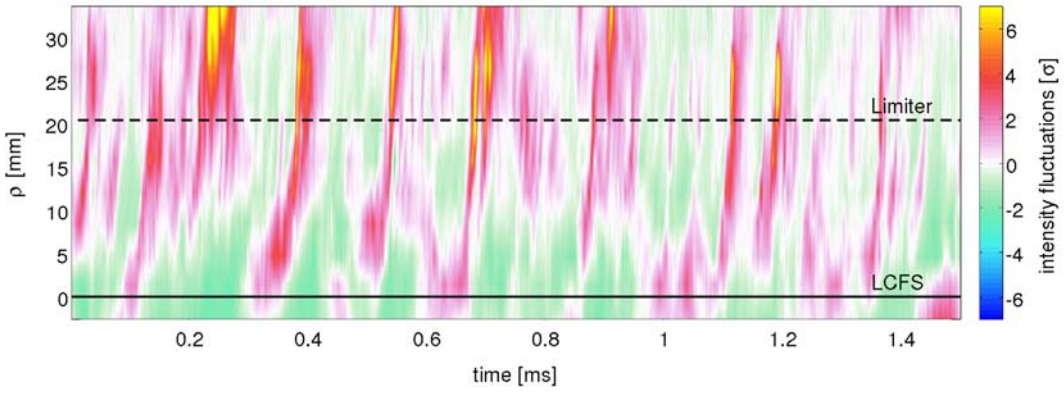

Fig. 1: Radial-temporal evolution of D_α intensity fluctuations normalized to standard deviation. ρ denotes the distance into the SOL. The LCFS and the limiter edge are explicitly shown.

radial array of fast D_α diodes which views the emission intensity across the SOL near the outer midplane is measured. The focal spot sizes are typically 4mm and long timeseries of fluctuations are recorded with high temporal resolution (1MHz sampling frequency). A typical radial-temporal evolution of the D_α intensity fluctuations (time-averaged emission is removed) as measured by the radial diode views is depicted in Fig. 1. Shown are the fluctuation time series normalized to the respective standard deviation σ for the different positions ρ across the SOL. The data are interpolated for better visibility. Large-amplitude positive fluctuation patterns with maximum fluctuation amplitudes of 6σ are observed. The patterns display an intermittent character with the occurrence of sporadic bursts. These bursts originate close to the LCFS, which is a region of strong radial plasma pressure gradient, and propagate through the entire SOL into the limiter shadow, where they decay. The radial propagation speed is not constant as it is easily seen from the changes of the inclination of the patterns. The radial velocity is generally smaller close to the LCFS. The bursts accelerate while propagating deeper into the SOL. The typical lifetime of the bursts is on the order of several 10μs. The fluctuation amplitudes are strongly asymmetric in time. No large negative fluctuation amplitudes are observed. At the LCFS events are observed that do not propagate into the SOL but disappear quickly.

As mentioned before the propagation of fluctuations is not purely in radial direction but also has a poloidal component. To investigate the propagation properties of the burst-like events in more detail, the D_α emission in the radial-poloidal plane is also viewed with a fast-framing camera. The camera records individual frames on a 64x64 pixel array with a frame rate of 250 kHz for the experiments presented here. The imaging optics allows for measurements in a plane spanning 6cm in poloidal and radial direction, covering the entire SOL width at the outer midplane and partly extending into the edge plasma. This makes it an ideal tool for the studies of the propagation features of fluctuations. The spatial resolution of the camera systems is ≈2mm in radial and poloidal direction. The camera's maximum storage is 300 frames, which results in a total record length of 1.2ms. For fluctuation analysis the time-averaged emission pattern is subtracted from each frame and the fluctuation time series of each individual pixel is normalized to its standard deviation. A sample measurement of the spatiotemporal evolution of a single long-living blob event is shown in Fig. 2. The four frames span over a time interval of 36μs. The blob evolution is consistent with the findings obtained with the radial array of diode views, Fig. 1. The blob forms close to the separatrix, its relative fluctuation amplitude increases while propagating into the SOL, and the blob decays in the limiter shadow. We note that the D_α intensity can not directly be attributed to

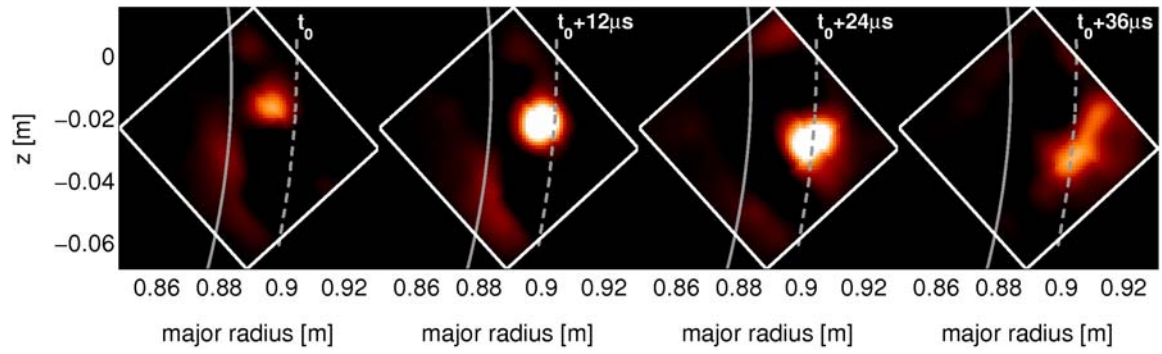

Fig. 2: Spatiotemporal evolution of D_α intensity fluctuations in the poloidal plane as measured with the fast framing camera over a time interval of 36μs. The LCFS is shown as solid line, the limiter shadow as dashed line. The fluctuation amplitude is color coded. White corresponds to large amplitudes, black to small.

the amplitude of plasma pressure fluctuations but is strongly affected by the spatial distribution of the neutral gas density from the gas puff and is a nonlinear function of electron density and temperature. The radial and poloidal extent of the blob are comparable with $l_r \approx l_p \approx 1$cm [11,12]. In contrast to the diode measurements the full two-dimensional dynamics of the blob is resolved. It is clearly visible that during outward propagation the blob also propagates downwards, which is in direction of the time-averaged ExB drift as measured by the reciprocating probe. Consistent with the diode measurements only large positive fluctuation amplitudes are observed.

3. Scales of SOL fluctuations

As has been emphasized before the SOL fluctuations are characterized by burst-like events, which amplitudes exceed by far the average fluctuation amplitude. This leads to non-Gaussian probability distribution functions (PDF), which develop large positive tails. To quantify the shape of the PDF the higher order moments skewness, *s* and kurtosis, *k* are calculated from the fluctuation time series of the radial array of diode views (for a Gaussian distribution we have $s=k=0$). The radial evolution across the SOL is shown in Fig. 3. The PDFs are always skewed towards positive values, indicating the developments of the large positive tails of the PDFs. The kurtosis shows relatively high positive values, which indicates peaked PDFs. Both moments are relatively constant from the LCFS (at $\rho=0$) to the limiter edge. Within the limiter shadow the values strongly increase and reach values of $s=3$ and $k=75$, respectively. This behavior is a direct consequence of the blob propagation into the limiter shadow, since the blob amplitude is by far larger than the time-averaged plasma density. These few, but large-amplitude events lead to large positive tails and strongly peaked PDF. Again, no indications for the contribution of large negative amplitude events to the PDFs are observed.

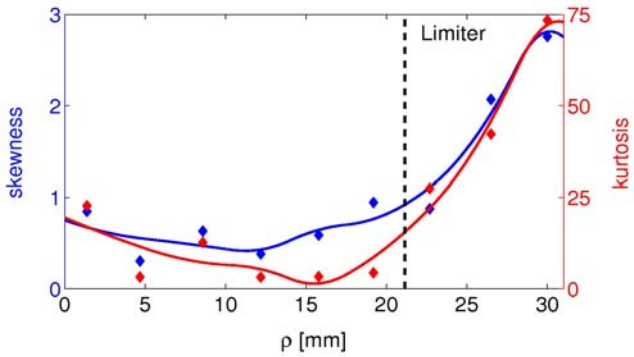

Fig. 3: Radial evolution of the higher order moments skewness and kurtosis of the PDF of D_α intensity fluctuations.

To quantify the spatial scales of SOL fluctuations we calculate the spectrum of the poloidal wavevector k_{pol} based on the camera recordings. To obtain the temporal development of k_{pol} we determine the wavevector spectrum on the basis of wavelet transform. We apply the

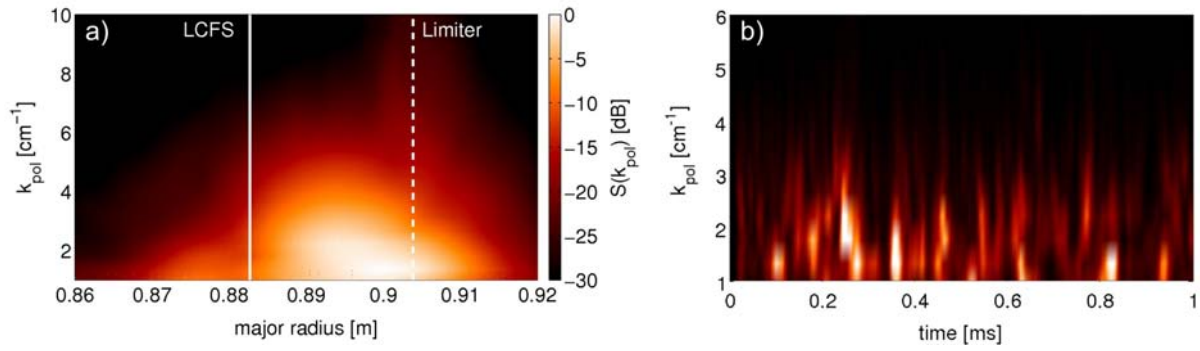

Fig. 4: Poloidal wavevector spectrum. a) Radial evolution of the poloidal wavevector power spectrum, averaged over the 1.2ms camera recording. b) Temporal evolution of the poloidal wavevector spectrum, averaged over all radial positions.

Morlet wavelet as base function, which has been found to be best applicable to the present data. The result of the calculation is shown in Fig. 4. The radial evolution of the k_{pol} spectrum, averaged over the camera record length is shown is Fig. 4(a). This is quite similar to what was found using Fourier techniques on multiple uncorrelated 2D "snapshots" of GPI emission [12]. Inside the LCFS the spectral power is relatively small. The power increases in the SOL, has a maximum in the mid-SOL, and decreases in the limiter shadow again. In the mid-SOL the spectrum peaks at small $k_{\_pol}$ with the maximum spectral power concentrated in the range $k_{\_pol} = 1.5 – 2.5 cm^{-1}$. This range corresponds to a typical structure size $a_b = \lambda/2 = \pi/k_{pol} = 1.2 – 2cm$. This is perfectly consistent with the size of the single event shown in Fig. 2. This characteristic structure size is found across the entire SOL gap and also partly in the limiter shadow. In the gap region also smaller scale structures contribute to the wavevector spectrum. Significant spectral power is found up to $k_{\_pol} = 5$, which corresponds to a structure size of ab = 0.6 cm. This finding demonstrates that the fluctuation spectrum is dominated by the blob events, which have a relatively large scale. The temporal evolution of $k_{\_pol}$ over almost the camera recording length of 1ms is shown in Fig. 4(b). For better statistics the spectra are averaged over the radius. We can observe the intermittent occurrence of few fluctuation events. The events have a typical lifetime of a few ten of μs. The characteristic spatial size of the events is similar to the dominant wavenumber, Fig. 4(a) with $k_{\_pol} = 1 – 2.5 cm^{-1}$. Thus, we can identify the events in the wavenumber spectrum as the blobs observed in the camera recordings. They dominate the evolution of the spectral power, the contribution of small-scale events is minor.

4. Radial propagation analysis

Inspection of the camera images, Fig. 2, revealed already the multidimensional propagation properties of blob events in the poloidal plane. To study the propagation in more detail we pursue a twofold approach: First, we analyze the propagation speed averaged over all amplitude and spatial scales. Second, we extract the large-amplitude fluctuation structures and evaluate their radial velocity. To obtain the scale-averaged poloidal and radial velocities we employ time delay correlation analysis. The cross-correlation function for each pixel time series, acting as reference time series, with all other pixel time series is calculated. This yields a two-dimensional correlation pattern for each reference time series. For a fixed time delay τ we determine the shift of the correlation maximum in radial Δr and poloidal Δp direction. The fluctuation velocity is then given by $v_r = \Delta r/\tau$, $v_p = \Delta p/\tau$. In the present analysis the time delay is chosen as $\tau = 8\mu s$, which is smaller than the correlation time of fluctuations. In this way we obtain the velocity field of fluctuations, which is averaged over time. The result for some of the pixels is shown in Fig. 5. Shown is the camera field-of-view (gray area) together with velocity vectors. The direction of the vectors indicate the direction of propagation, their respective lengths the propagation speed (in arbitrary units). Four

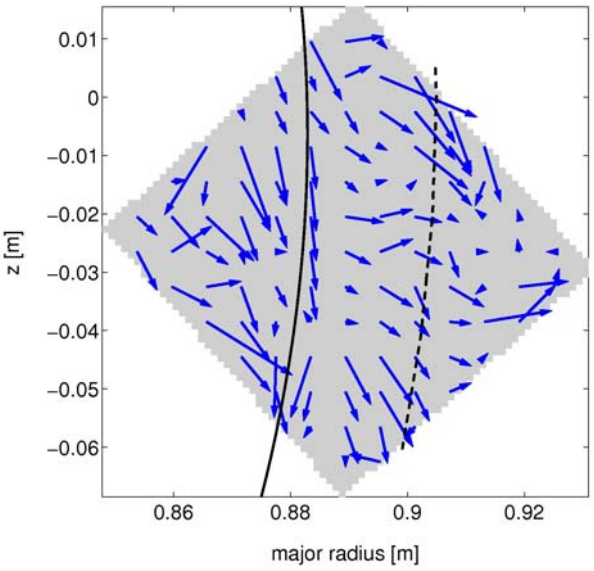

Fig. 5: Two-dimensional velocity field based on time delay correlation analysis of D_α intensity fluctuations of the camera images. The arrows give direction and their respective length the magnitude of propagation speed.

different regions of propagation characteristics can be distinguished. Within the LCFS the observed propagation speeds are generally approx. a factor of two higher than in the SOL and have a strong radial and poloidal component. Close to the separatrix the velocity is mainly in poloidal direction in direction of the ion polarization drift. While penetrating into the SOL the poloidal velocity components decreases and fluctuations propagate mainly in radial direction. Only close to the edge of the camera's field of view at a major radius of R≈ 0.9m a significant poloidal propagation speed is observed. The poloidal component becomes stronger again at the limiter shadow while the radial speed remains essentially unchanged.
Interestingly, we do not observe the change of mean poloidal fluctuation velocity close to the LCFS, where the ExB background velocity changes direction.
Also within the LCFS the poloidal propagation is mainly downwards, i.e. in ion diamagnetic drift direction, as in the SOL. The reason for the discrepancy between background ExB drift direction and fluctuation velocity is yet not completely clear. It has been observed that the poloidal fluctuation velocity might be strongly influenced by an intrinsic mode velocity [13], which leads to deviations from the ExB drift velocity. Another possible effect is aliasing. Due to the relatively small poloidal observation range plasma fluctuations with large poloidal velocity (> 3km/s) can sometimes propagate out of the camera‘s field of view within the chosen time lag. Thus, we can in such a case not reliably track the correlation maximum of fluctuations, which then would cause artificially high velocity components in radial and poloidal direction. This issue is, however, restricted to the plasma inside the separatrix.
The poloidal velocities observed at the separatrix are much larger than the radial ones, which is consistent with the strong poloidal velocity shear usually found here. Within the SOL the poloidal velocity is much smaller than the radial velocity and fluctuations propagate essentially in radial direction, thereby contributing strongly to the cross-field transport. The poloidal velocity becomes more distinct in the limiter shadow. This is probably a consequence of the radial electric field changing, since here it is strongly influenced by the limiter boundary condition. In the SOL we obtain average values for the poloidal velocity of v_p = 250 m/s and for the radial velocity v_r = 170 m/s, which corresponds to ≈0.3% of the local ion sound speed. The findings are consistent with the one-dimensional analysis based on the array of diode views. Events are found to have higher radial velocities in the mid-SOL when compared to the LCFS position. The strong poloidal propagation component at the LCFS leads to rapid poloidal displacement of structures, which are not tracked with the radial diode views and appear as events only at the LCFS. The derived velocity fields and the observations about them are consistent with those based on a similar, but not identical, time-delay cross-correlation analysis of the sequential camera images, as described in [14].
The correlation analysis is independent of spatial or amplitude scale. To specifically investigate the radial propagation of blob events, we decompose the camera images into blobs of different amplitude scales and track the blobs within the field of view over the camera frames. Similarly to the correlation analysis the spatial displacement of the blobs within two frames together with the time delay of the frames yields the radial blob velocity. Since only a few blob events are observed in one camera recording we combine the camera data of four identical discharges to

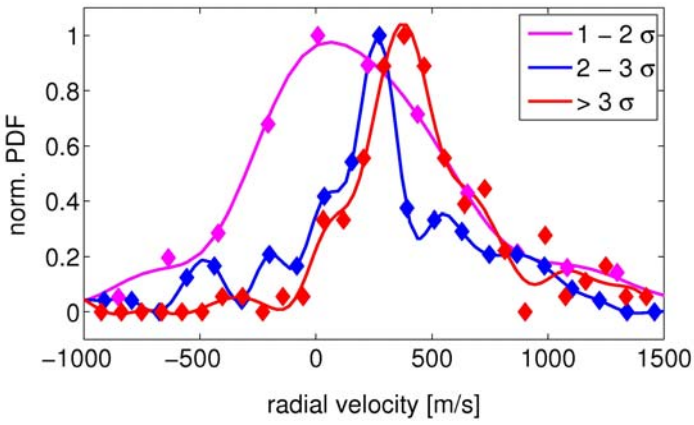

Fig. 6: Normalized PDFs of the radial blob velocities for three different peak blob amplitudes

improve statistics. We calculate normalized PDFs for the radial velocity component, which then yields the mean structure velocity. The result is depicted in Fig. 6. Shown are the PDFs of the radial velocities for blob events with peak amplitudes within three different ranges: peak amplitudes between 1σ - 2σ (R1), between 2σ - 3σ (R2), and blobs with amplitudes exceeding 3σ (R3). Over the four discharges typically 50 events for each amplitude condition are collected. For all conditions the PDF's center positions are shifted towards positive velocities, which corresponds to outward radial propagation in this representation. For condition R1 the distribution is relatively broad with some events reaching $v_r > 100$ m/s. The center position is found at a velocity of $v_r = 130$ m/s, which corresponds roughly to the mean velocity obtained from the correlation analysis. Interestingly, the mean radial velocity increases with an increase of the peak blob amplitude. For condition R2 the distribution function becomes narrower and a mean radial velocity of $v_r = 227$ m/s is found. Finally, for condition R3, peak of the PDF is shifted further and the corresponding mean radial velocity id $v_r = 430$ m/s. This finding clearly demonstrates that the radial blob velocity is a function of the blob amplitude with the general tendency that larger amplitude blobs propagate faster outwards. All mean velocities are significantly smaller than 10% of the local ion sound speed, which corresponds to 5km/s. In comparison with the correlation analysis we obtain similar radial velocities for the low amplitude blobs. This finding together with the relatively narrow size range observed in the poloidal wavevector spectra strongly suggests that correlations in the SOL are predominantly caused by blob events.

Although a direct quantitative comparison with model predictions based on the present data has not yet been done for this data, we can compare the predicted trend. Using blob propagation models that are based on interchange dynamics, it was shown that the radial blob velocity increases with the relative blob fluctuation degree as $v_r/c_s \sim (\delta p/p_0)^{1/2}$, where c_s is the ion sound speed and $\delta p/p_0$ is the blob amplitude relative to background p_0 [15]. Since the time-averaged SOL profiles are the same for the present experiments, the increase of the peak blob amplitude corresponds to an increase in blob fluctuation degree. We can experimentally confirm the increase of radial velocity with relative fluctuation degree. If we assume that larger peak blob amplitudes correspond to larger blob sizes, our observations are in contradiction to blob polarization models in the sheath connected regime, which predict an increase of the radial blob velocity with decreasing blob size [16]. However, with its high SOL plasma densities in C-Mod and associated high collision frequencies, the C-Mod SOL is not in the sheath-connected regime.

5. Summary

We have presented observations of the propagation properties of fluctuation structures in the SOL of Alcator C-Mod using gas-puff imaging diagnostics. These diagnostics show a clear radial propagation of fluctuation events with large positive amplitudes. The events lead to PDFs that deviate strongly from a Gaussian and develop large positive tails. We have not observed any negative fluctuation events anywhere in the SOL. The poloidal wavevector spectrum analyzed on the basis of wavelet transform shows a distinct large-scale range dominating the spectral power, which corresponds to structure sizes of 1.2 – 2 cm. The temporally resolved wavevector spectrum shows the intermittent occurrence of spectral features in time, which can be identified as the blob events observe with the fast framing camera. Correlation analysis yields the velocity field of fluctuations in the SOL. A shear layer close to the LCFS is clearly observed. In the mid-SOL fluctuations propagate predominantly in radial direction, thereby contributing strongly to the fluctuation-induced cross-field transport. Restriction of the radial velocity analysis to blob events with different peak

amplitudes revealed that larger amplitude blobs propagate faster radially. This trend is in general agreement with the proposed scaling based on interchange mode drive.

Acknowledgements

F. Brochard is kindly acknowledged for fruitful discussions about wavelet analysis of camera data. One author (O.G.) thanks the Alexander-von-Humboldt foundation for financial support for the experimental campaign. This work is support by Department of Energy Coop. Agreement DE-FC02-99ER54512 and DE-AC02-76CHO3073.

References

[1] D'Ippolito, D.A., et al., "Cross-field blob transport in tokamak scrape-off layer", Phys. Plasmas, 9(1), 222–233, 2002.
[2] Boedo, J.A., et al., "Transport by intermittent convection in the boundary of the DIII-D tokamak", Phys. Plasmas, 8:11, 2001.
[3] Boedo, J. A., et al., "Transport by intermittency in the boundary of the DIII-D tokamak", Phys. Plasmas, 10(5):1670–1677, 2003.
[4] Grulke, O., et al., "Radially propagating fluctuation structures in the scrape-off layer of Alcator C-mod", Phys. Plasmas, 13:012306–1 – 012306–7, 2006.
[5] Carter, T., "Intermittent turbulence and turbulent structures in a linear magnetized plasma", Phys. Plasmas, 13:010701–1 – 010701–4, 2006.
[6] Yu, G.Q., et al., "Dynamics of blobs in scrape-off layer/shadow regions of takamaks and linear devices", Phys. Plasmas, 10(11):4413–4418, 2003.
[7] D'Ippolito, D.A., et al., "Rotational instability of plasma blobs", Phys. Plasmas, 11(10):4603–4609, 2004.
[8] Garcia, O.E., et al., "Computations of intermittent transport in scrape-off layer plasmas", Phys. Rev. Lett., 92(16):165003–1 – 165003–4, 2004.
[9] Terry, J.L., et al., "Visible imaging of turbulence in the SOL of the Alcator C-Mod tokamak", J. Nucl. Mater., 290-293:757–762, 2001.
[10] Maqueda, R.J., et al., „Edge turbulence measurements in NSTX by gas puff imaging", Rev. Sci. Instrum., 72(1):931–934, 2001.
[11] Zweben, S.J., et al., „Edge turbulence imaging in the Alcator C-Mod tokamak", Phys. Plasmas, 9(5):1981–1989, 2002.
[12] Terry, J.L., et al., "Observations of the turbulence in the scrape-off layer of Alcator C-Mod and comparisons with simulation", Phys. Plasmas, 10(5):1739–1747, 2003.
[13] Fenzi, C., et al., "Effect of ion ∇B drift direction on density fluctuation poloidal flow and flow shear", Phys. Plasmas, 12:062307–1 – 062307–9, 2005.
[14] Terry, J.L., et al., "Velocity fields of edge/scrape-off-layer turbulence in Alcator C-mod", J. Nucl. Mater., 337-339:322–326, 2005.
[15] Garcia, O.E., et al., "Mechanism and scaling for convection of isolated structures in nonuniformly magnetized plasmas", Phys. Plasmas, 12:090701–1 – 090701–4, 2005.
[16] Myra, J.R., et al., "Blob birth and transport in the tokamak edge plasma: analysis of imaging data", in preparation.